INTERNATIONAL JOURNAL FOR NUMERICAL METHODS IN ENGINEERING, VOL. 23, 1313–1328 (1986)

A LINEAR THICK CURVED BEAM ELEMENT

C. RAMESH BABU AND G. PRATHAP

Structural Sciences Division, National Aeronautical Laboratory, Bangalore 560017, India

SUMMARY

Early attempts to derive curved beam and shell elements in a curvilinear system were dramatically unsuccessful. This was wrongly attributed to the failure of these elements to recover strain-free rigid body displacement modes in a curvilinear co-ordinate description. Recent evidence points to a 'membrane locking' phenomenon that arises when constrained strain fields corresponding to inextensional bending are not 'consistently' recovered. This accounts for, more completely and precisely, the failure of such elements.

In this paper, a simple linear two-noded C^0 continuous thick curved beam element based on a curvilinear deep shell theory is derived free from shear and membrane locking. Lack of consistency in the shear and membrane strain-field interpolations in their constrained physical limits (Kirchhoff and inextensional bending limits, respectively) causes very poor convergence due to locking and severe spurious oscillations in stress predictions. Error estimates for these are made and verified. Field-consistent strain interpolations remove these errors and produce the most efficient linear element possible.

INTRODUCTION

The history of the finite element method reveals clearly that curved beam and shell elements based on curvilinear geometry have been singularly difficult to design. Even when these have been produced using 'artifices' such as reduced integration, selective integration, discontinuous force field hybrid and mixed methods or the addition of incompatible bubble modes, they have been very difficult to rationalize.

The earliest attempts to design a thin curved beam based on the simplest shape function representation admissible, i.e. a C^0 continuity for the tangential displacement u and a C^1 continuity for the normal displacement w, ended inexplicably in failure.[1,2] Characteristic of this failure was the need to have a very large number of these elements (henceforth, the cubic–linear or CL element) to produce accurate solutions — requirements of element lengths of the order of the thickness of the shell were clearly very unreasonable. What made this even more inexplicable was the fact that an idealization with straight line beam elements based on the same cubic–linear fields could achieve acceptable accuracy with many fewer elements; a fact which continues to receive much attention even today.[3–5]

Two unrelated mechanisms have been offered, in the literature, as explanations. The first was the need to secure a satisfactory description of the rigid-body displacement modes in a strain-free manner. It was argued that simple displacement fields expressed in curvilinear co-ordinates cannot represent rigid-body motions in a Cartesian frame unless the trigonometric functions that couple the translations are accommodated *a priori*. Straight line elements seem to be free of this requirement, and this, it was believed, accounted for the clear superiority of this representation.

The second requirement was the need to recover 'sensitive' solutions.[6] These are low energy inextensional bending solutions which can be recovered without perturbations only if polynomial displacement fields in which the tangential displacement, u, is exactly one order higher than the

0029–5981/86/101313–16$08.00 *Received 29 July 1985*

radial displacement, w, are used. However, this argument fails to explain why cubic–linear straight line elements perform well, as the sensitivity requirement projects a cubic–quartic representation for these displacements. Further, the two requirements were conflicting — coupled transcendental or trigonometric functions for one and polynomials for the other, suggesting that either coupled fields with both trignometric and polynomial fields, or that independent polynomial fields of high order will meet both requirements.

Armed with these rules, a great deal of experimentation with curved beams has taken place without a very definitive picture emerging. At the time of the most comprehensive survey of these developments to date,' it would appear that the constant strain element' was the simplest and most efficient derived so far. It couples the u and w fields by adding trigonometric functions meant to satisfy the rigid-body displacement requirement to polynomial fields of quadratic u and linear w meant to satisfy the 'sensitivity' requirement. This produced a constant membrane and linear bending strain element that showed the most superior convergence in displacements of elements of its class, and axial forces that were accurate and free of any kind of spurious oscillations. In stark contrast to this, Dawe[9] needed very high order independent polynomial interpolations for u and w (quintic–quintic being typical) to produce good convergence in displacements, but this element could still show violent oscillations in the axial force distribution. A new conceptual scheme was apparently needed to resolve all this.

Some recent evidence[10–14] indicates that the rule about the need for transcendental coupling to ensure strain-free rigid body motion in a curvilinear system may have been wrongly emphasized. It seems unnecessary to ensure that curvilinear-based descriptions must identically reproduce Cartesian-based translations and rotations. Meck[10] showed that the use of polynomial, but coupled, displacement fields that ensured a state of inextensionality produced a very well behaved element — the 'sensitive' solutions were accommodated by this but not the transcendental coupling required for strain-free rigid body motion in Cartesian-co-ordinate-based systems.

Noor and Peters,[11] working with the same element we study here, showed that exact integration of the membrane energy terms produced a very poor element. This was incorrectly attributed to the supposed inability of this element to represent strain-free rigid body modes. A magnification of errors in inextensional energy terms by a factor proportional to the square of the ratio of the radius of curvature of the element to its thickness was also observed, but it was not clear how this error emerged from the strain-free rigid-body motion requirement. A reduced integration of the membrane strain energy dramatically freed the element of these errors. Since reduced integration actually smooths and reduces the order of polynomial fields used to represent the displacements, this should make errors due to lack of strain-free rigid body motion, if any, even more significant, whereas exactly the opposite was found.

In independent investigations, Belytschko and Stolarski'[12] and Prathap and Bhashyam[13] successfully proposed the concept of a 'membrane locking' phenomenon to explain the very poor behaviour of exactly integrated low order independently interpolated polynomial field curved beam elements. Prathap[14] showed that 'membrane locking' originated from the inability of these simple interpolations to produce a membrane strain field that can vanish in a 'consistent' way so that only true inextensional constraints are enforced in physical limits where this becomes an important consideration, e.g. the 'sensitive' problems. The CL element was re-examined on this basis and error models derived, which could predict, quantitatively, the nature of the error and its manner of propagation. It was also shown that by the 'trick' of integrating the membrane strain energy so that only a 'consistent' true constraint remained, the CL1 element (1 indicating a one-point Gaussian integration of membrane strain energy) of Reference 14 was the most efficient simple thin curved beam element that could be envisaged.

In this paper, we re-examine the Noor and Peters[11] element from the viewpoint of field-

consistency concepts.[15,16] This starts with independent linear interpolations for the three field variables needed for a curved beam with shear deformation: the tangential displacement u, the radial displacement w, and the section rotation θ. However, the membrane strain field and the shear strain field are derived indirectly from these in a redistributed way using strain smoothing, so that each strain field is 'consistent'—the constant membrane, bending and shear strain element that results will be the most efficient element of this class. We shall show that if this redistribution is not done, then the 'field-inconsistent' elements will have both shear and membrane locking, and will yield wildly oscillating shear and membrane stresses. These oscillating stresses are the mechanisms by which the very high spurious additional stiffness of locking is incorporated within each element in the form of strain energy. Error estimates for these are derived. A series of specially constructed numerical experiments confirms these projections.

THE LINEAR CURVED BEAM

The strain energy of a curved beam of length 2l, taking into account the effect of transverse shear deformation, can be written as the sum of its membrane, bending and shear energy terms as

$$U = U_M + U_B + U_S \tag{1}$$

where

$$\begin{aligned} U_M &= \int_{-l}^{l} \tfrac{1}{2} EA(u_{,x} + w/R)^2 \, dx \\ U_B &= \int_{-l}^{l} \tfrac{1}{2} EI(\theta_{,x} - u_{,x}/R)^2 \, dx \\ U_S &= \int_{-l}^{l} \tfrac{1}{2} kGA(\theta - w_{,x})^2 \, dx \end{aligned} \tag{2}$$

In equations (2), u, w and θ are the tangential and radial displacements and section rotation. E and G are the Young's and shear moduli and k is the shear correction factor. I, A and R are the moment of inertia, the cross-sectional area and the radius of curvature. In these exercises, the radius of curvature, R, is taken as a constant for each element. However, in general applications, I, A and R can be interpolated in specified ways over the element length. These strain energies correspond to extensional, flexural and shear strains of the form

$$\varepsilon = u_{,x} + w/R \tag{3a}$$

$$\chi = \theta_{,x} - u_{,x}/R \tag{3b}$$

$$\gamma = \theta - w_{,x} \tag{3c}$$

These equations are based on a curvilinear co-ordinates system, with x measured along the arc.

The field-inconsistent element

The conventional procedure is to start with a linear isoparametric representation of the field variables u, w and θ. The interpolation functions

$$\begin{aligned} N_1 &= (1 - \xi)/2 \\ N_2 &= (1 + \xi)/2 \end{aligned} \tag{4}$$

are used. The dimensionless co-ordinate $\xi = x/l$ varies from -1 to $+1$ for an element of length $2l$. The strain energies in equations (2) are now directly computed, in an analytically or numerically exact way, using these interpolation functions in the expressions for the strain fields, equations **(4).**

We shall now examine, from the field-consistency point of view,[15,16] the implications of this approach. Starting from linear interpolations based on equations (4), we can associate two constants with each of the field variable interpolations in the following manner:

$$\begin{aligned} u &= a_0 + a_1(x/l) \\ w &= b_0 + b_1(x/l) \\ \theta &= c_0 + c_1(x/l) \end{aligned} \tag{5}$$

These lead to the following interpolations for the strain fields in terms of these constants:

$$\varepsilon = (a_1/l + b_0/R) + (b_1/R)(x/l) \tag{6a}$$

$$\chi = (c_1/l - a_1/Rl) \tag{6b}$$

$$\gamma = (c_0 - b_1/l) + c_1(x/l) \tag{6c}$$

An exact evaluation of the strain energies of the element will now give

$$U_M = \tfrac{1}{2}(EA)(2l)\{(a_1/l + b_0/R)^2 + \tfrac{1}{3}(b_1/R)^2\} \tag{7a}$$

$$U_B = \tfrac{1}{2}(EI)(2l)\{(c_1/l - a_1/Rl)^2\} \tag{7b}$$

$$U_S = \tfrac{1}{2}(kGA)(2l)\{(c_0 - b_1/l)^2 + \tfrac{1}{3}c_1^2\} \tag{7c}$$

In the respective constraining physical limits, the membrane and shear energies are critical. Thus, in inextensional bending, the membrane energy must vanish in a 'consistent' way, i.e. the constants that define this in equation 7(a) must accommodate this limit by producing the correct constraints, and in the Kirchhoff limit corresponding to classical thin beam behaviour, the shear strain energy must vanish again in a 'consistent' fashion. An examination of the conditions produced by this requirement shows that the following constraints would emerge in these limits:

$$a_1/l + b_0/R \to 0 \tag{8a}$$

$$c_0 - b_1/l \to 0 \tag{8b}$$

$$b_1/R \to 0 \tag{8c}$$

$$c_1 \to 0 \tag{8d}$$

In our terminology,[15,16] constraints (8a) and (8b) are field-consistent, as they contain, in each case, constants from all the contributing field variables relevant to that strain field. The constants can then accommodate the true inextensional and Kirchhoff constraints in a physically meaningful way. Equations (8c) and (8d) contain, in each case, only a term from one of the contributing field variables. A constraint imposed on these will lead to undesirable restrictions on each of these field variables. We shall show below how these constraints lead to 'shear locking' and 'membrane locking' and to violent disturbances in the evaluation of axial thrust and shear force.

The field-consistent element

We can formulate a field-consistent element, free of these deficiencies, in many ways. The 'trick' is to evaluate the membrane and shear strain energies so that only the consistent terms will

contribute to the membrane and shear strain energies. This can be done by simply dropping the undesirable terms from equations (7a) and (7c). Or this can be achieved by using a reduced integration rule, i.e. a Gaussian one-point integration of shear and membrane energy will produce the same result.[14,17] Other techniques such as the addition of bubble modes with nodeless variables, the hybrid and mixed methods, can produce the same result if the manipulations are done judiciously; otherwise they too will be ineffective.

In this paper, we propose that a field-consistent redistribution for the shear and membrane strain fields can be obtained if we use substitute shape functions

$$\bar{N}_1 = \bar{N}_2 = 1/2$$

for the w field variable in the membrane strain expression, (3a) and for the θ field variable in the shear strain expression, (3c). This substitute shape function can be thought of as a least squares smoothed equivalent of the original linear interpolations to make the field variables involved, w and θ, field-consistent with the $u_{,x}$ and $w_{,x}$ terms that appear in equations (3a) and (3c), respectively. With such an interpretation, the shear and membrane strain energies can be evaluated by any order of integration. This is useful, especially where a high order of integration may be needed for tapered beams. The order of integration is therefore freed from the field-consistency requirement. There is also no ambiguity about the actual thrust and shear force evaluations—these come directly from the field-consistent strain fields, are valid over the whole element and do not show the violent fluctuations seen from a field-inconsistent formulation.

LOCKING AND STRESS OSCILLATIONS

Shear locking in a field-inconsistent element

It is simple to derive the shear locking present through the functional reconstitution technique established for the straight Timoshenko beam.[13] The mathematical operations of the discretization process, i.e. the definition of a small but non-infinitesimal element of length 2l, the use of the field-inconsistent interpolations and an exact evaluation of all energies, will result in an element that models a spuriously stiffened beam. Consider a nealy straight beam (i.e. large R) of length L. It has an energy functional

$$\pi = \int_0^L \tfrac{1}{2} EI\theta_{,x}^2 \, dx + \int_0^L \tfrac{1}{2} kGA(\theta - w_{,x})^2 \, dx \tag{9}$$

If an element of length 2l is isolated, the discretization process produces an energy for the element of the form (see equations (7))

$$\pi_e = \tfrac{1}{2}(EI)(2l)\theta_{,x}^2 + \tfrac{1}{2}(kGA)(2l)(\theta - w_{,x})^2 + \tfrac{1}{2}(kGAl^2)(2l)(\theta_{,x}^2/3) \tag{10}$$

where the constants in equation (7) which appear in the discretization process have been reconstituted into their original continuum form as contributing field variables. From this reconstituted functional, we can consider that an idealization of a beam region of length 2l into a linear finite element would produce a modified energy density within that region,

$$\pi_e' = \tfrac{1}{2}(EI + kGAl^2/3)\theta_{,x}^2 + \tfrac{1}{2} kGA(\theta - w_{,x})^2 \tag{11}$$

In other words, the reconstituted functional for the whole beam is

$$\pi' = 1/2 \int_0^L EI(1 + kGAl^2/3EI)\theta_{,x}^2 \, dx + 1/2 \int_0^L kGA(\theta - w_{,x})^2 \, dx \tag{12}$$

We now have a representation that is stiffer than the undiscretized beam by the factor $kGAl^2/3EI$. For a very thin beam, this can be very large, and produces the additional stiffening effect known as 'shear locking'. We can demonstrate that this simple error model predicts shear locking exactly by observing that a nearly straight beam discretized in this way would produce an error defined by the additional stiffness parameter norm'[8]

$$e = (w(\text{theory})/w(\text{FEM}) - 1) = kGAl^2/3EI \tag{13}$$

This will be confirmed later in a numerical experiment.

Membrune locking in a field-inconsistent element

A *similar* operational procedure, as done for the shallow curved beam[13] and for the deep arch element,[14] will show that in a curved beam, there is an additional spurious energy term of the form

$$\frac{1}{2}\int_0^L (EAl^2/3R^2)w_{,x}^2 \, dx \tag{14}$$

This amounts to the generation of a spurious stiffening in-plane force field that causes the 'membrane locking'. In the shear locking case earlier, the modification was simple, as the flexural rigidity was directly altered and an exact estimate for the error norm could be made. In this case, however, the modification enters as a complex interaction between the spurious in-plane stiffening force field and the other energy terms. Therefore, an estimate of the error norm in terms of a constant C (e.g. C = 1/3 for shear locking in equation **(13))** does not seem to be straightforward. However, it is possible to establish the form of the structural parameters that induce locking and which will appear in the error norm, by observing that the stiffening mechanism here is identical to that for a shallow curved Timoshenko beam[13] and for a deep arch element.[14] The very crude simplifications made in Reference **14** for a very shallow arch (or nearly straight beam) show that an error norm of the form

$$e_m = C(l/t)^2 \, (L/R)^2 \tag{15}$$

is operative, where (l/t) gives half the element length-to-thickness ratio and (L/R) gives the length of arch to radius of curvature. These are measures of its thinness and deepness — membrane locking becomes more severe for thinner and deeper arches. We shall confirm that this error norm is valid in numerical experiments later.

Axial thrust and shear force evaluation

The elegance of the field-consistent redistribution for membrane and shear strains will become evident when we compare the axial thrust N and shear force V obtained from the original field-inconsistent representations with those obtained from the field-consistent interpolations, which we shall call $\bar{N}$ and $\bar{V}$. From equations (6), these are

$$\bar{N} = EA(a_1/l + b_0/R) \tag{16a}$$

$$\bar{V} = kGA(c_0 - b_1/l) \tag{16b}$$

$$N = \bar{N} + EA(b_1/R)(x/l) \tag{16c}$$

$$V = \bar{V} + kGA(c_1)(x/l) \tag{16d}$$

N and V have linear terms that relate directly to the constants that appear as the spurious

constraints in equations (8c) and (8d). These terms will appear as violent spurious oscillations in the axial thrust and shear forces. *A priori* estimates for the maghitudes of these oscillations can be made for special cases and confirmed by numerical experiments. This will establish that field-inconsistency operating through the spurious constraints is the source of these oscillations. In other words, the oscillating stress fields are the manifestation of the spurious additional energies of stiffening that cause locking.

On the other hand, the field-consistent shear and axial forces are constant values throughout the element. These values can also be interpreted as the values of these stresses sampled at the centroid of the element, and this lends justification to the use of the centroid as the single integrating point in the reduced integration scheme.

We shall now derive estimates of these oscillations in a very simple example which will be used later for numerical experimentation.

Shear force in a nearly-straight beam with tip-moment

The straight cantilever beam has a concentrated moment applied at the free end. This should produce a constant moment M and a zero shear force V through the length of the beam. An element of length $2l$ at any station on the beam will now respond in the following manner. If the element is field-consistent, we can associate the constant c_1, after accounting for discretization, to relate to the bending moment M at the element centroid, from equation (6b) as

$$c_1 = Ml/EI \tag{17a}$$

In a field-inconsistent problem, owing to shear locking, we need to consider the modified flexural rigidity, so that

$$c_1 = (Ml/EI)/(1 + e_s) \tag{17b}$$

where $e_S = kGAl^2/3EI$.

The field-consistent element will respond with $\bar{V} = \mathbf{0}$. The field-inconsistent shear force V, from equations (16d) and (17b) can be written as

$$V = \{(kGA)(Ml/EI)/(1 + e_S)\}(x/l) \tag{18}$$

If the beam is very thin so that $e_S \gg 1$, we obtain

$$V = (3M/l)(x/l) \tag{19}$$

These are violent shear force oscillations, within each element, that originate directly from the field-inconsistency in the shear strain definition. It is seen that these oscillations are independent of the element thickness when $e_S \gg 1$, but become more violent with smaller elements! This will be confirmed in a numerical example in the next section.

From this simple example, it is possible to project that, in more complex examples, the use of field-inconsistent elements will lead to oscillating shear force fields

$$V = V_0 + \{(kGA)(M_0 l/3EI)/(1 + e_S)\}(x/l) \tag{20}$$

where V_0, M_0 are the shear force and bending moment at the centroid of the element.

Axial force in a nearly-straight cantiliver beam with tip-moment

To isolate the membrane locking phenomenon alone, we shall consider a nearly-straight cantilever beam (i.e. R large enough to reproduce straight beam results but small enough to

introduce curved beam effects) and model it with elements which are already field-consistent in shear. An element that is also field-consistent in membrane strain will respond with

$$\bar{N} = -M/R \tag{21}$$

which follows from the simple in-plane force equilibrium equation for a curved element, and

$$V = \bar{V} = kGA(c_0 - b_1/l) = 0 \tag{22}$$

Thus $b_1 = c_0 l$ can be related to θ_0, the rotation at the centroid of the element, as $b_1 = c_0 l = \theta_0 l$. An element that is field-inconsistent in membrane-strain will therefore show, from equation (16c),

$$N = \bar{N} + (EA\theta_0 l/R)(x/l) \tag{23}$$

These show up as violent oscillations within the element, originating from the term that is spuriously constrained in equation (8c). It does not appear to be possible to relate the oscillations to the bending moment M appearing at the centroid of the element, as was done for the shear force in equation (20) earlier. This is because the additional stiffening effect represented by equation (14) is produced in a complex manner by the linearly-varying stress-fields of equation (23) which interact with the other energy terms. However equation (23) shows that from the computed values of θ, at the CMCS element centroids, it is possible to predict the extent of the oscillations. Such an envelope can be confirmed through numerical experiments to show that the present conceptual scheme is verifiable.

NUMERICAL EXPERIMENTS

For a critical evaluation of the present theory, the following element variations are chosen for study:

(i) CMCS—field-consistent membrane and shear strains
(ii) CMIS—field-consistent membrane and field-inconsistent shear strains
(iii) IMCS—field-inconsistent membrane and field-consistent shear strains
(iv) IMIS—field-inconsistent membrane and shear strains.

In all cases, the stiffness matrix is obtained by a two-point Gaussian integration of all energy terms. In each case, the forces and moments are evaluated directly at the nodes so that the oscillations, where present, could be identified. These elements were then tested through a series of numerical examples so that the various predictions made earlier could be confirmed.

Test case 1: locking in a nearly straight cantilever beam

A cantilever beam of length $L = 10$ in. and width $b = 1$ in. is taken to be nearly straight, i.e. R of the order of 10^3 in. and very thin, t of the order of 10^{-3} in. A vertical load is applied at the free end. The beam is idealized with 1 to 6 and 10 elements of all four variations of the element. The manner in which the structural parameters influence locking is examined by carrying out three sets of control experiments. In the first set, $R = 10^3$ in., $t = 10^{-3}$ in. and l is varied, corresponding to 1 to 6 and 10 elements of equal length. In the second set, $t = 10^{-3}$ in. and $l = 1{\cdot}667$ in., corresponding to $N = 3$ elements; R is varied from 10^3 in. to 5×10^3 in. In the third set, $R = 10^3$ in. and $l = 1{\cdot}667$ in.; t is varied from 10^{-3} in. to 5×10^{-3} in. In all cases, the error norm is computed as

$$e = (w(\text{theory})/w\ (\text{FEM}) - 1)$$

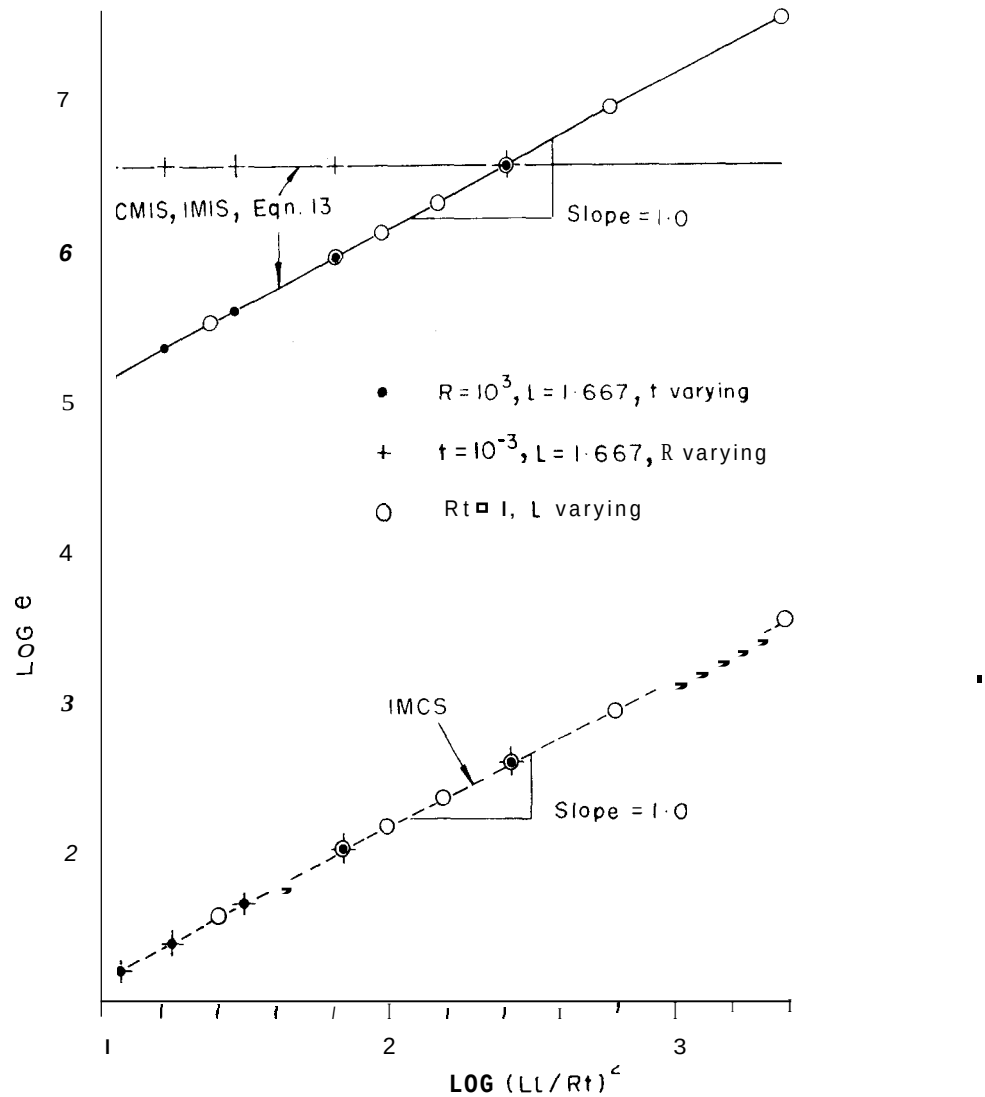

Figure 1. Locking in a nearly straight cantilever beam

where w is the deflection at the tip of the cantilever.

The results are plotted on the logarithmic scale, as shown in Figure 1. In all the cases considered, the error norm e for the **CMCS** idealization ranged from Log $e = -0.48$ to -2.56 and was too small to be shown in the range given in Figure 1. It was also seen that these values of e depended only on the element length l (or number of elements N) and were virtually independent of the structural ratios (l/t) and (L/R). Thus, in the nomenclature of Reference 18, these are errors of the first kind that vanish quickly with element size and are indifferent to changes in the structural multipliers.

The finite element results from all three other models show very large errors. The **IMCS** results for all three sets of control experiments show that the error of the second kind propagates exactly in the $(Ll/Rt)^2$ fashion described by equation (15). The error norms for the **CMIS** and **IMIS** element models are virtually identical, showing that the error due to shear locking is very much larger than the error due to membrane locking in the **IMIS** element. When the values of $k = 5/6$ and $\nu = 0.3$ are substituted into equation (13), the error model predictions, indicated by the solid lines in Figure 1 are in very accurate agreement with the error norm computed from the finite

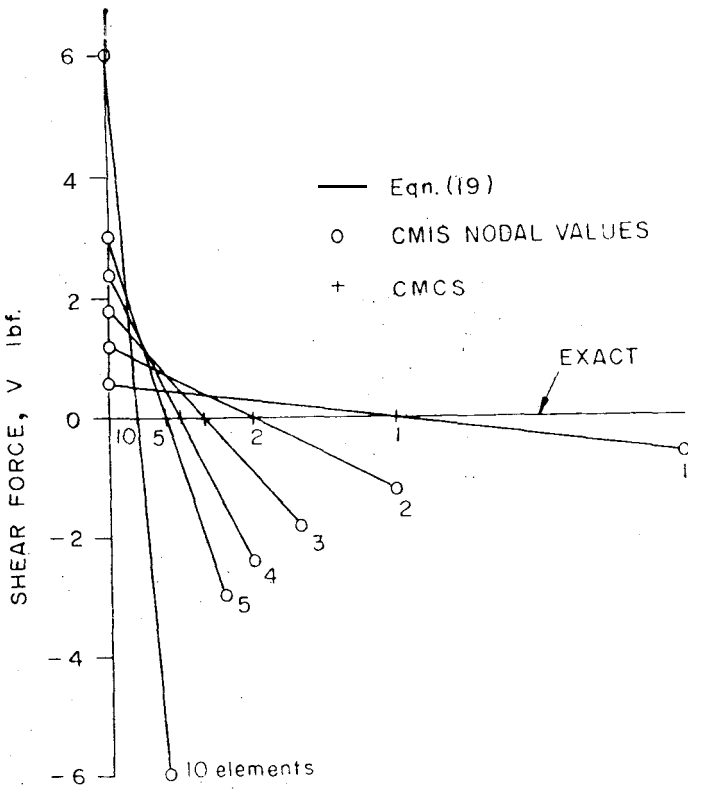

Figure 2. Shear force oscillations in a cantilever beam with tip moment

element results, Of special interest is the case where R is varied—e_S is now indifferent to this variation, confirming the absence of the effect of R in shear locking as seen from equation (13).

Test case 2: nearly-straight cantilever beam with tip-moment

The beam has the following dimensions: $L = 10$ in., $R = 10^3$ in., $b = 1$ in. and $t = 10^{-3}$ in. A tip-moment of -1 lbf.in. is applied. The elastic properties are $E = 10^7$ lbf/in^2., $\nu = 0.3$ and $k = 5/6$. An idealization with one **CMCS** element produces, very accurately, the straight beam result, i.e. $\theta = 0{\cdot}12 \times 10^5$ and $w = 0{\cdot}6 \times 10^5$ in., as this element can model the constant bending moment exactly. This one element solution also produces the axial force exactly, i.e. $N = -M/R = 10^{-3}$ lbf, showing that the field-consistent element recovers the equilibrium in the axial direction correctly.

We shall now examine the stress oscillations that emerge when field-inconsistent elements are used. Figure 2 shows the shear forces evaluated at the nodes of the CMIS element models. In each case, only the variation over the first element is shown, as the pattern repeats itself identically over all other elements. This follows from the error model prediction in equation (19), as the moment is a constant over all elements. It is seen that the finite element results are predicted very accurately by equation (19), shown by the solid lines in the Figure. It is also seen that the oscillations become more severe when the element lengths are reduced.

Figure 3 shows the oscillations in the axial force field when 10 **IMCS** elements are used to model the beam. Node 1 corresponds to the tip and Node 11 to the fixed end. The circles indicate the nodal values obtained from the finite element output. The solid lines are the values predicted by the error model, (23), with θ, now being taken as the value at the element mid-point from the same finite element output. The excellent agreement confirms the error model. The oscillations are seen to decay rapidly, from the tip to the fixed end, in an exponential fashion, and this in turn is reflected by

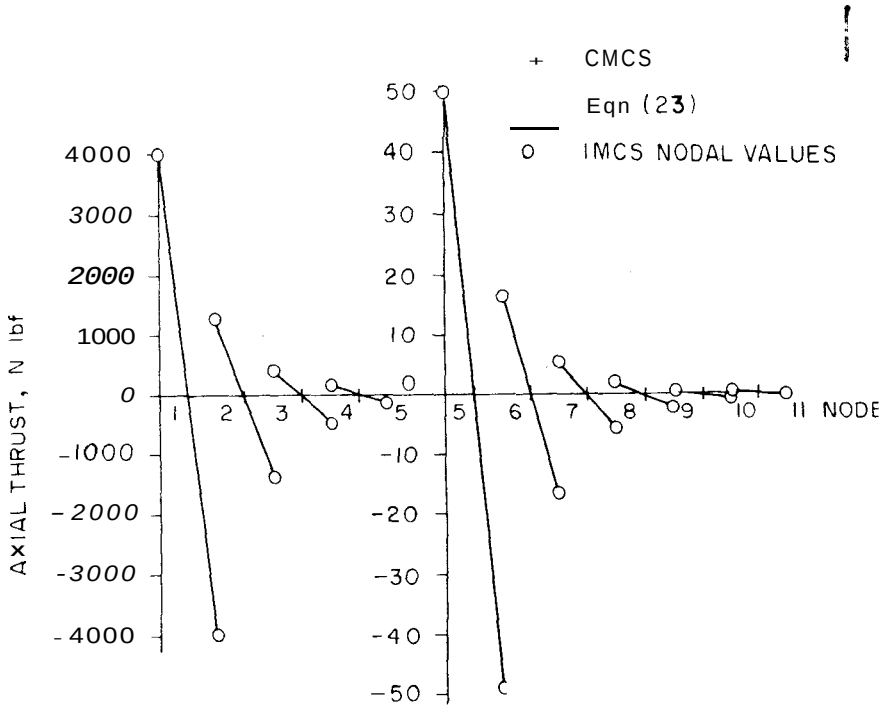

Figure 3. Membrane force oscillations in a cantilever beam with **tip** moment

the exponential decay in θ as one approaches the fixed end. Note that this pattern differs drastically from the true picture, where θ should vary linearly from the fixed end to the tip. The exponential pattern of decay is typical of structures stiffened by large in-plane forces.

Test case 3: pinched ring

A pinched ring serves as the best illustration to demonstrate the behaviour of these elements in a deep arch configuration (Figure 4). An exact solution for the radial deflection under the load w_A; and for the bending moment, shear force and axial force at any station ϕ from the vertical, can be easily derived from elementary energy principles. For a ring with $R = 4{\cdot}953$ in., $t = 0.094$ in., b = 1 in., $E = 10{\cdot}5 \times 10^6$ lbf/in.^{2}, $\nu = 0.3125$ and with pinching loads $P = 100$ lbf. at points **A** and C, we have

$$w_A = 1.244 \text{in.} \tag{24a}$$

$$M(\phi) = PR[(2/\pi) - \sin\phi]/2 \tag{24b}$$

$$N(\phi) = -(P/2)\sin\phi \tag{24c}$$

and

$$V(\phi) = (P/2)\cos\phi \tag{24d}$$

All four variations of the linear element are used to model the quadrant from A to **B** with 2 to 6 and 10 elements. Figure 5 shows the convergence trend for the radial deflection w_A, on a logarithmic scale. It is seen that the CMCS element models show very rapid convergence to the correct answer. The other three element types show very poor convergence. With 10 elements, the IMCS, CMIS and IMIS element models show deflections which are more than an order of magnitude away from the correct answer. The dramatic improvement seen in the CMCS element has resulted entirely from the removal of shear and membrane locking.

Figure 6 compares the finite element results for the bending moment distribution along the

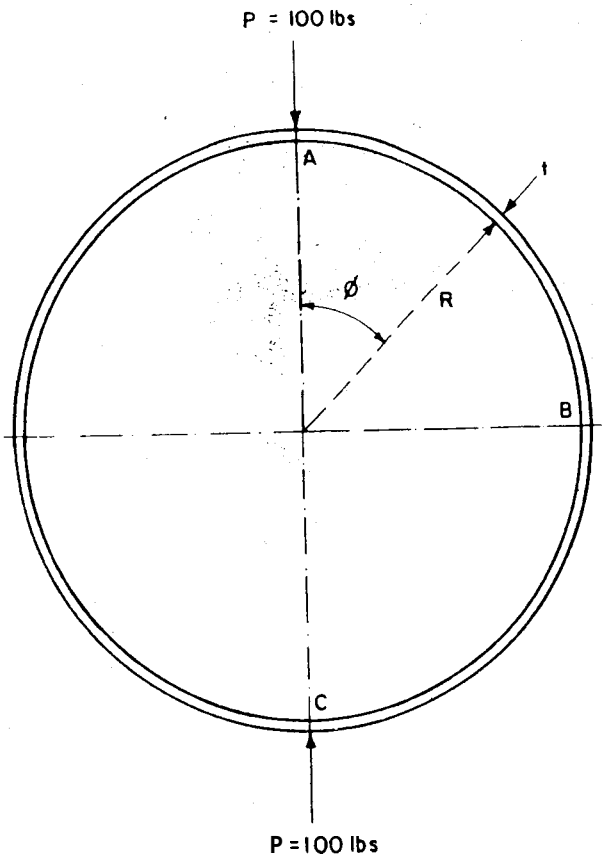

Figure 4. Pinched ring

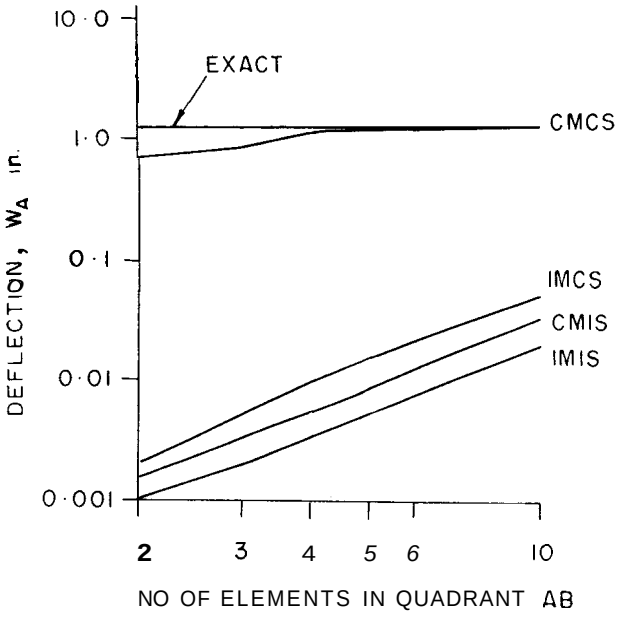

Figure 5. Convergence of radial deflection under load for a pinched ring

quadrant **AB** with the theoretical prediction of equation (24b). Since each **CMCS** element gives constant bending moment over the element length, this value is indicated on Figure 6 at element

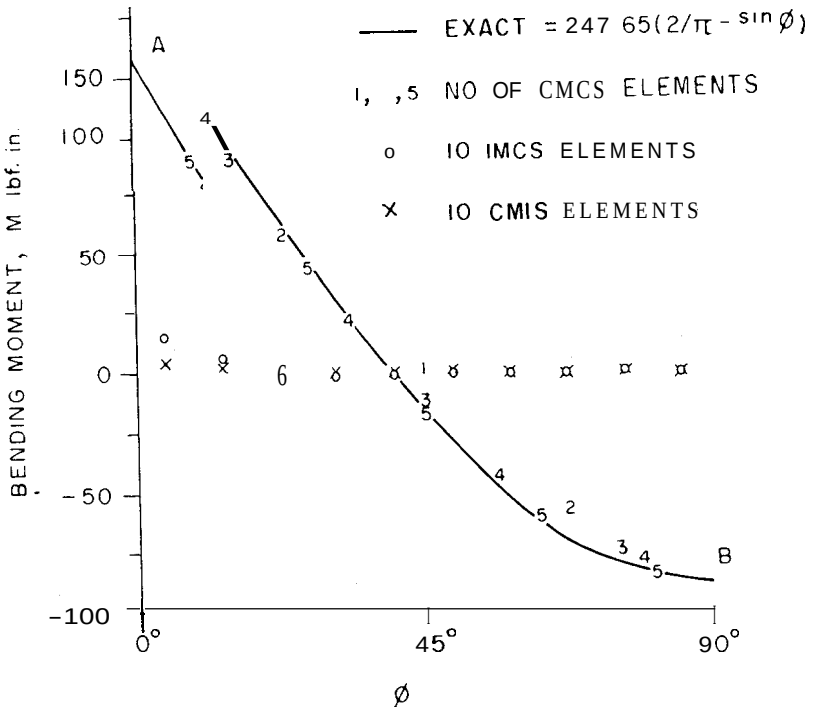

Figure 6. Bending moment in a quadrant of a pinched ring

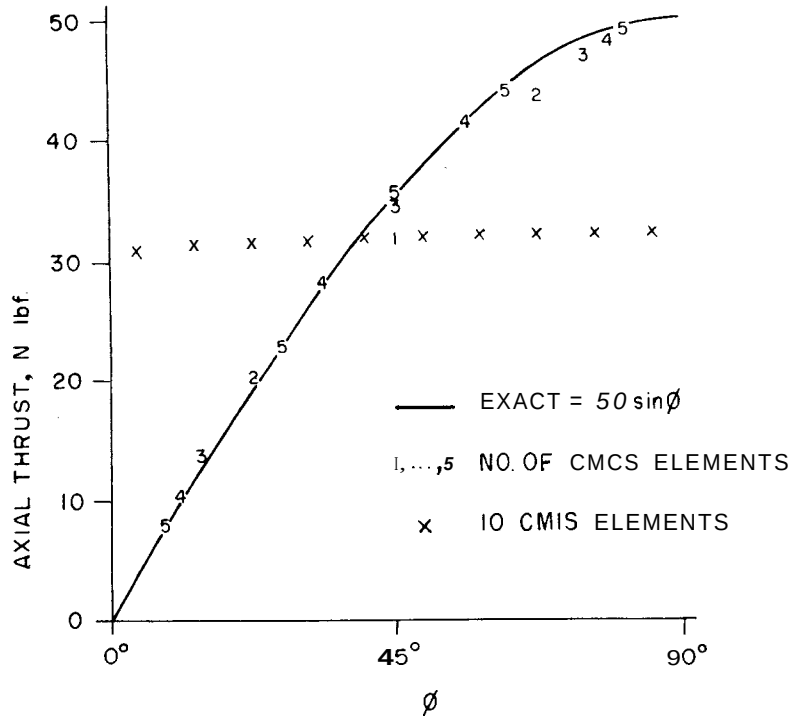

Figure 7. Axial thrust in a quadrant of a pinched ring with CMCS elements

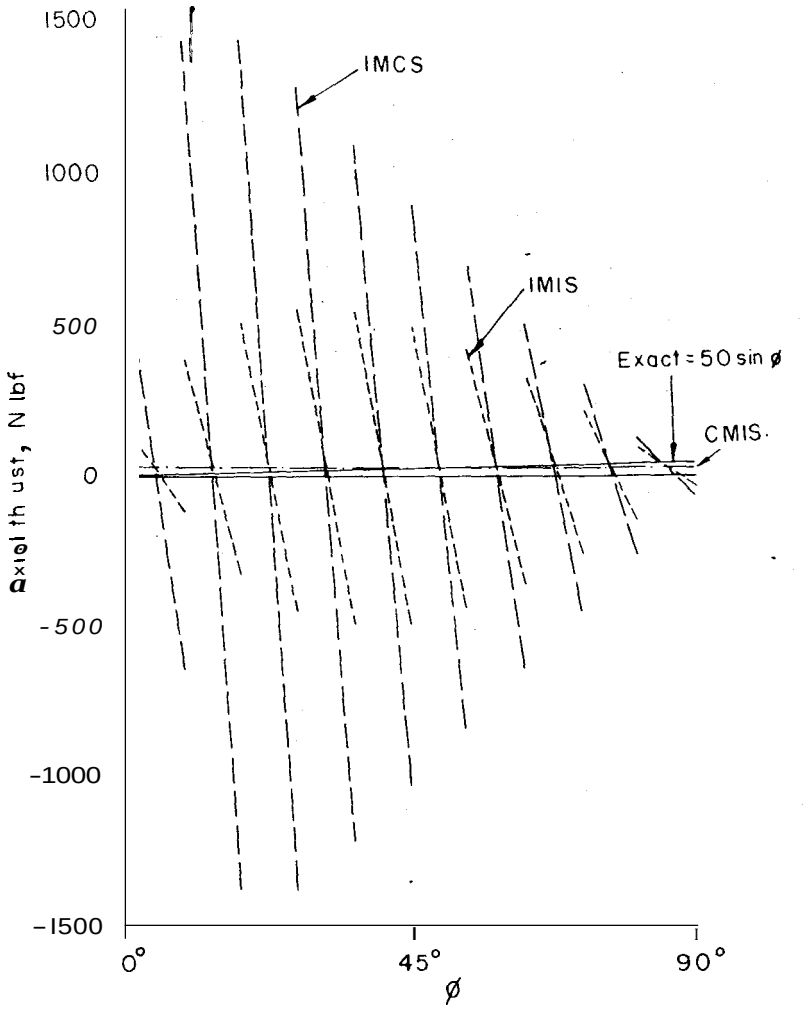

Figure 8. Axial thrust in a quadrant of a pinched ring— 10 element idealization

mid-points; the number indicating the model from which the result is taken. It is seen that the CMCS results converge very rapidly to the correct values. However, the IMCS and CMIS elements show that the stiffening errors due to membrane and shear locking are very large and result in moments which are an order of magnitude too low, even with 10 elements. The **IMIS** results, not shown here, are lower than the CMIS results, and reflect the combined action of membrane and shear locking.

Figure 7 compares the finite element results for the axial thrust distribution along **AB** with the theoretical result in equation (24c). Again, the CMCS element models behave very well. The oscillations resulting from the IMCS and IMIS elements are too violent to be shown here and will be drawn to a different scale in the next Figure. Interestingly, the **CMIS** idealization produces a nearly constant value of axial force, varying from 31.0 to 32·2 lbf over the quadrant as a result of the stiffening due to the shear locking alone.

The shear force results from the CMCS element models behave in as almost identical fashion to the axial force distributions and are similarly accurate. This follows from the fact that the shear force distribution seen from equation (24d) is complementary to the axial force distribution of equation (24c). The CMIS and IMIS models yield violent shear force oscillations and are not shown here. The IMCS element idealization produces **a** shear force distribution that varies smoothly from 30·2 to 0·03 lbf over the quadrant, reflecting the stiffening due to membrane

locking and the absence of stress oscillations due to field-consistency in shear strain.

Figure 8 shows, on a different scale, the orders of magnitude involved in the stress oscillations produced by field-inconsistency in the membrane strain field in the IMCS and IMIS element models. The oscillations from the IMIS element models are less pronounced, due to the additional stiffening of shear locking.

CONCLUSIONS

The simplest C^0 continuous linear thick curved beam is derived free of shear and membrane locking by using field-consistent shear and membrane strain interpolations. The locking errors and spurious oscillations due to field-inconsistency have been studied and, where possible, a **priori** error models are derived and confirmed through numerical experimentation. It is also clear that early apprehensions about errors resulting from the supposed lack of strain-free rigid body motion in such elements were incorrect and that such errors can be completely accounted for by the membrane locking phenomenon.

It is possible to derive the same field-consistent element by other techniques. If bubblemodes of a quadratic nature are added to w and θ with additional nodeless degrees of freedom and these are then condensed out, the element that results will be a similar to this. The Noor and Peters element" achieves the same result by a reduced integration strategy and sampling stresses only at the mid-point of the element.

The hybrid or mixed methods based on complementary energy, Hellinger–Reissner or Hu–Washizu theorems can be shown to be indirect methods of smoothing out the field-inconsistent strain interpolations. If the assumed stresses correspond to the inconsistent strain fields derived from the displacement fields, then locking and stress oscillations will remain even in the hybrid/mixed methods. However, if the assumed stresses are chosen carefully as to cover only the consistent parts of the constrained strain fields, the element so obtained will be identical to a field-consistent displacement model. Thus, a hybrid/mixed element that starts with linear fields for the displacements and rotations and constant moment, shear force and axial thrust as the assumed stress fields, will produce an element identical to the **CMCS** element. The additional mathematical operations and complexity that follow from a hybrid/mixed formulation do not justify its use when the same results are achieved more neatly and quickly by the use of a ***priori*** field-consistent redistributions of the strain fields within the context of a displacement type formulation.

ACKNOWLEDGEMENTS

The authors are deeply indebted to Dr. B. R. Somashekar, Head, Structures Division, for his constant interest and encouragement. The authors are grateful to Prof. G. Subramanian, Indian Institute of Technology, Madras for his useful discussions and suggestions in improving the quality of this paper.

REFERENCES

1. **K. H.** Murray, 'Comments on the convergence of finite element solutions', ***A.I.A.A.J.*,4,** 815–816 (1966).
2. **J.** E. Walz, R. E. Fulton, N. J. Cyrus and R. **T.** Eppink, 'Accuracy of finite element approximations to structural problems', ***NASA TN-D*** 5728 (1970).
3. **F.** Kikuchi, 'Accuracy **of** some finite element models **for** arch problems', ***Comp. Meth. Appl. Mech. Eng.*, 35, 315-345** (1982).
4. Y. Yamamoto and **H.** Ohtsubo, 'A qualitative accuracy consideration on arch elements', *Int.* **j. numer.** ***methods eng.*, 18,** 1179–1195 (1982).

5. F. Kikuchi and K. Tanizawa, 'Accuracy and locking-free property of the beam element approximation for arch problems', *Comp. Struct.*, **19,** 103–110 (1984).
6. L. S. D. Morley. 'Polynomial stress states in first approximation theory ofcircular cylindrical shells', Q. *J. Mech. Appl. Math., 25,* 13–43 (1972).
7. D. G. Ashweil and R. H. Gallagher, (eds), ***Finite Elements for Thin Shell and Curved Members,*** Wiley, London, 1976.
8. D. G. Ashwell, A. B. Sabir and T. M. Roberts, 'Further studies in the application of curved finite elements to circular arches', *Int. J. Mech. Sci.*, 13, 507–517 (1971).
9. D. J. Dawe, 'Some higher order elements for arches and shells' in D. G. Ashwell and R. H. Gullagher (eds), ***Thin Shells and Curved Members*** Wiley, London, 1976, chap. 8, pp. 131–153.
10. H. R. Meck, 'An accurate polynomial displacement function for finite ringelements', *Comp. Struct.*, **11,** 256–269 (1980).
11. A. K. Noor and J. M. Peters, Mixed models and reduced/selective integration for curved elements', *Int. j. numer. methods eng.*, 17, 615–631 (1981).
12. H. Stolarski and T. Belytschko, 'Membrane locking and reduced integration for curved elements', *J. Appl. Mech.,* **49,** 172–178 (1981).
13. G. Prathap and G. R. Bhashyam, 'Reduced integration and the shear flexible beam element', *Int. j. numer. methods eng.,* **18,** 195–210 (1982).
14. G. Prathap, 'The curved beam/deep arch/finite ring element revisited, *Int. j. numer. methods eng.,* **21,** 389–407 (1985).
15. G. Prathap, 'Field consistent finite element formulations', *Interner Bericht IB 131–84/33,* DFVLR Institut fur Strukturmechanik, Braunschweig, W. Germany (1984).
16. G. Prathap, 'Field consistency and the finite element analysis of multi-field structural problems' in ***Analysis of Structures*** K. A. V. Pandalai and B. R. Somashekar (eds), NAL-SP-RPT-1/84, Bangalore, India, 1984.
17. T. J. R. Hughes, R. L. Taylor and W. Kanoknukulchai, 'A simple and efficient finite element for plate bending', *Int. j. numer. methods eng.*, 11, 1529–1543 (1977).
18. G. Prathap, 'An additional stiffness parameter measure of errors of the second kind in the finite element method', *Int. j. numer. methods eng.,* **21,** 1001–1012 (1985).